

M-5

DOT/FAA/CT-82/83

# Application of Thermochemical Modeling to Aircraft Interior Polymeric Materials

Won Dokko  
Kumar Ramohalli

Jet Propulsion Laboratory  
California Institute of Technology  
Pasadena, California 91109

June 1982

Final Report

This document is available to the U.S. public through the National Technical Information Service, Springfield, Virginia 22161.



US Department of Transportation  
**Federal Aviation Administration**  
Technical Center  
Atlantic City Airport, N.J. 08405



National Aeronautics  
and Space Administration

US 8350 8W  
~~US 3750~~

## NOTICES

This document was prepared by the Jet Propulsion Laboratory, California Institute of Technology, and was sponsored by the Federal Aviation Administration, U.S. Department of Transportation through an agreement with NASA.

This document is disseminated under the sponsorship of the Federal Aviation Administration, Department of Transportation in the interest of information exchange. The United States Government assumes no liability for the contents or use thereof.

The United States Government does not endorse products or manufacturers. Trade or manufacturer's names appear herein solely because they are considered essential to the object of this report.

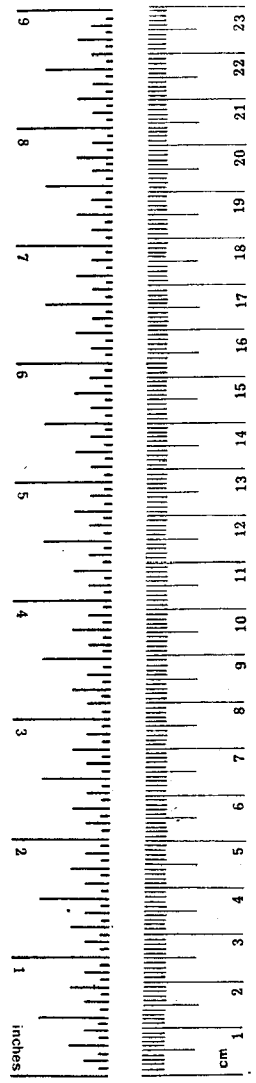
1. Report No. DOT/FAA/CT-82/83		2. Government Accession No.		3. Recipient's Catalog No.	
4. Title and Subtitle Application of Thermochemical Modeling to Aircraft Interior Polymeric Materials				5. Report Date June 1982	
				6. Performing Organization Code	
7. Author(s) Won Dokko, Kumar Ramohalli				8. Performing Organization Report No. JPL 5030-543	
9. Performing Organization Name and Address Jet Propulsion Laboratory California Institute of Technology Pasadena, California 91109				10. Work Unit No. (TRAIS)	
				11. Contract or Grant No. DOT-FABONA	
12. Sponsoring Agency Name and Address U.S. Department of Transportation Federal Aviation Administration Technical Center Atlantic City Airport, New Jersey 08405				13. Type of Report and Period Covered Final Report 5/30/80 - 5/30/81	
				14. Sponsoring Agency Code	
15. Supplementary Notes					
16. Abstract This report summarizes the results from a twelve-month study of the feasibility of applying certain basic concepts in thermochemical modeling to aircraft cabin fire safety. The concepts developed earlier on a NASA-sponsored program were applied to six specific tasks dealing with the thermochemical performance of interior carpets and seat cushions. The specific objective was to predict the burning rate as a function of the material property values, geometry and heat flux; more important, it was the aim to predict and provide rationale for certain special features that have been experimentally observed by the FAA. It was also the specific objective to introduce new concepts that have not been the subject of pursuit at other centers. That is, the novel concepts developed at JPL were highlighted. Three fundamental hypotheses were introduced: the condensed phase degradation of the polymeric material is the overall rate-limiting step; the extent of degradation at the vaporization step (at the surface) is not arbitrary but has to be specified by a scientific criterion such as the vapor pressure equilibrium criterion; and the diffusion/mixing of the pyrolysis products with the oxidizer (air) is the rate-limiting step in the vapor phase combustion. The results indicate that the assumption of condensed-phase reaction as the rate-limiting step is correct, that the thermochemical performance can be predicted using the ingredient properties only, and that a certain theoretical result predicted by this model is in qualitative agreement with experimental observations. For example, it is predicted that a typical carpet can not burn under its own flame but needs augmentation by an external radiation source for sustained burning, and this was observed experimentally.					
17. Key Words Thermochemical modeling, aircraft interior materials, wool carpet, polyurethane foam, burning rate, effect of flame-retardant, effect of pressure, Spalding-B number, thermal thickness				18. Distribution Statement	
19. Security Classif. (of this report) Unclassified		20. Security Classif. (of this page) Unclassified		21. No. of Pages	22. Price

## METRIC CONVERSION FACTORS

### Approximate Conversions to Metric Measures

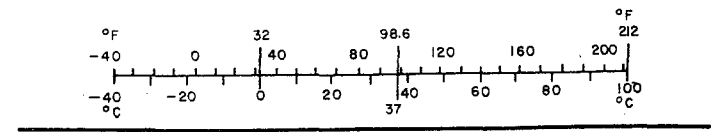
Symbol	When You Know	Multiply by	To Find	Symbol
<b>LENGTH</b>				
in	inches	*2.5	centimeters	cm
ft	feet	30	centimeters	cm
yd	yards	0.9	meters	m
mi	miles	1.6	kilometers	km
<b>AREA</b>				
in <sup>2</sup>	square inches	6.5	square centimeters	cm <sup>2</sup>
ft <sup>2</sup>	square feet	0.09	square meters	m <sup>2</sup>
yd <sup>2</sup>	square yards	0.8	square meters	m <sup>2</sup>
mi <sup>2</sup>	square miles	2.6	square kilometers	km <sup>2</sup>
	acres	0.4	hectares	ha
<b>MASS (weight)</b>				
oz	ounces	28	grams	g
lb	pounds	0.45	kilograms	kg
	short tons (2000 lb)	0.9	tonnes	t
<b>VOLUME</b>				
tsp	teaspoons	5	milliliters	ml
Tbsp	tablespoons	15	milliliters	ml
fl oz	fluid ounces	30	milliliters	ml
c	cups	0.24	liters	l
pt	pints	0.47	liters	l
qt	quarts	0.95	liters	l
gal	gallons	3.8	liters	l
ft <sup>3</sup>	cubic feet	0.03	cubic meters	m <sup>3</sup>
yd <sup>3</sup>	cubic yards	0.76	cubic meters	m <sup>3</sup>
<b>TEMPERATURE (exact)</b>				
°F	Fahrenheit temperature	5/9 (after subtracting 32)	Celsius temperature	°C

\*1 in = 2.54 (exactly). For other exact conversions and more detailed tables, see NBS Misc. Publ. 286, Units of Weights and Measures, Price \$2.25, SD Catalog No. C13.10:286.



### Approximate Conversions from Metric Measures

Symbol	When You Know	Multiply by	To Find	Symbol
<b>LENGTH</b>				
mm	millimeters	0.04	inches	in
cm	centimeters	0.4	inches	in
m	meters	3.3	feet	ft
m	meters	1.1	yards	yd
km	kilometers	0.6	miles	mi
<b>AREA</b>				
cm <sup>2</sup>	square centimeters	0.16	square inches	in <sup>2</sup>
m <sup>2</sup>	square meters	1.2	square yards	yd <sup>2</sup>
km <sup>2</sup>	square kilometers	0.4	square miles	mi <sup>2</sup>
ha	hectares (10,000 m <sup>2</sup> )	2.5	acres	
<b>MASS (weight)</b>				
g	grams	0.035	ounces	oz
kg	kilograms	2.2	pounds	lb
t	tonnes (1000 kg)	1.1	short tons	
<b>VOLUME</b>				
ml	milliliters	0.03	fluid ounces	fl oz
l	liters	2.1	pints	pt
l	liters	1.06	quarts	qt
l	liters	0.26	gallons	gal
m <sup>3</sup>	cubic meters	35	cubic feet	ft <sup>3</sup>
m <sup>3</sup>	cubic meters	1.3	cubic yards	yd <sup>3</sup>
<b>TEMPERATURE (exact)</b>				
°C	Celsius temperature	9/5 (then add 32)	Fahrenheit temperature	°F



## PREFACE

The work described in this report was performed by the Jet Propulsion Laboratory, California Institute of Technology, and was sponsored by the Federal Aviation Agency through an agreement with the National Aeronautics and Space Administration. The authors would like to thank Dr. Thor Eklund, the FAA Project Manager, Messrs. Constantine Sarkos, Wayne Howell, and Richard Kirsch of the FAA and Allen Tobiason of NASA for their suggestions and support.

TABLE OF CONTENTS

<u>Chapter</u>		<u>Page</u>
1.	<u>INTRODUCTION</u> . . . . .	1
2.	<u>GENERAL APPROACH</u> . . . . .	1
	(a) Condensed Phase Details . . . . .	2
	(b) Gas Phase Details . . . . .	4
	(c) Model Predictions . . . . .	5
3.	<u>SUPPORTING EXPERIMENTS</u> . . . . .	5
	(a) Kinetics Constants . . . . .	5
	(1) <u>Wool Carpet</u> . . . . .	5
	(2) <u>Seat Cushion (Polyurethane Foam)</u> . . . . .	7
	(b) Other Data . . . . .	12
4.	<u>SPECIFIC TASKS IN THE INTERAGENCY AGREEMENT</u> . . . . .	12
	(a) Burning Rates Under Flaming and Non-flaming Conditions . . . . .	12
	(1) <u>Carpet</u> . . . . .	12
	(2) <u>Seat Cushion</u> . . . . .	18
	(b) Effects of Chemical Fire Retarding Agents on Burning Rate . . . . .	18
	(c) Integration of the Nomenclature: "Thermal Thickness" and "Thermal Thinness" . . . . .	21
	(d) Relating the Vaporization Concept to the Spalding B Number . . . . .	24
	(e) Effect of Pressure on Burning Rates . . . . .	26
5.	<u>CONCLUSIONS</u> . . . . .	27
6.	<u>FUTURE WORK</u> . . . . .	27

<u>Chapter</u>	<u>Page</u>
REFERENCES . . . . .	30
APPENDIX A - Computer program for calculations for seat cushion. . . . .	A-1
APPENDIX B - Computer program for calculations for carpet. . . . .	B-1
APPENDIX C - Experimental DSC data . . . . .	C-1
APPENDIX D - Experimental TGA data . . . . .	D-1

LIST OF FIGURES

<u>Figure</u>		<u>Page</u>
1	Thermochemical Model For Condensed Phase Degradation Under Sheet Flame . . . . .	3
2	Thermogravimetric Analysis Of Carpet Fibers . . . . .	6
3	Reaction Rate Of Carpet Fibers Deduced From TGA . . . . .	8
4	SEM Pictures Of Carpet Fibers . . . . .	9
5	TGA Analysis of Seat Cushion . . . . .	10
6	Reaction Rate For Seat Cushion Deduced From TGA . . . . .	11
7	Predicted Burning Rate Of Carpet With Incident Heat Flux. . .	15
8	Predicted Burning Rate Of Carpet . . . . .	17
9	Carpet Under Self-Sustaining Flame . . . . .	19
10	Predicted Burning Rate Of Seat Cushion . . . . .	20
11	Predicted Effect Of Flame-Retardant On The Burning Of Carpet . . . . .	22
12	Predicted Effect of Flame-Retardant On The Burning Of Seat Cushion . . . . .	23
13	Schematic Diagram For The Condensed Phase Burning With Convective Flow . . . . .	25
14	Pressure Dependence Of Burning Rate of Carpet . . . . .	28
15	Pressure Dependence of Burning Rate of Seat Cushion . . . . .	29

LIST OF TABLES

<u>Table</u>		<u>Page</u>
1	Arrhenius Constants Obtained From TGA Experiments . . . . .	13
2	Basic Data Used In The Calculations . . . . .	14

## NOMENCLATURE

B	Pre-exponential constant for thermal degradation ( $\text{sec}^{-1}$ )
$c_{\text{gas}}$	Specific heat of vapor phase, at constant pressure ( $\text{cal gm}^{-1}\text{C}^{-1}$ )
c	Specific heat of solid polymer ( $\text{cal gm}^{-1}\text{C}^{-1}$ )
$c^{-}, c^{+}$	A point immediately above and below the charring temperature $T_c$ , respectively
D	Energy for complete depolymerization of polymer ( $\text{cal gm}^{-1}$ )
E	Activation energy for thermal degradation of polymer ( $\text{cal mole}^{-1}$ )
FSC	Number of monomer units of degraded polymer at charring temperature
FSV	Number of monomer units in a statistically averaged vaporizing fragment at the surface
k	Thermal conductivity coefficient ( $\text{cal cm}^{-1} \text{sec}^{-1}\text{C}^{-1}$ )
$k_l, k_h$	Thermal conductivity of charred and uncharred material, respectively
L	Thickness of material (cm)
m	Mean mass of vaporizing species at the surface (gm)
M	Mean molecular weight of vaporizing species at the surface ( $\text{gm g-mole}^{-1}$ )
N	Number of bonds in the polymer at any location normalized with respect to the number in the unaffected state.
P	Mean pressure of the system (atm)
$q''_s$	Surface heat flux from vapor phase ( $\text{cal cm}^{-2} \text{sec}^{-1}$ )
R	Universal gas constant ( $\text{cal g-mole}^{-1} \text{K}^{-1}$ )
r	Linear regression rate of polymer solid ( $\text{cm sec}^{-1}$ )
t	Time (sec)
T	Temperature (K)
$T_b$	Time-averaged peak temperature in vapor phase (K)
$T_c$	Charring temperature (K)
$T_0$	Initial temperature (K)
$T_s$	Surface temperature (K)

$x$	Distance coordinate normal to the surface (cm)
$x^*$	Flame standoff distance (cm)
$U_{\text{gas}}$	Flow velocity (cm sec <sup>-1</sup> )
$\alpha$	Thermal diffusivity (cm <sup>2</sup> sec <sup>-1</sup> )
$\delta$	Thermal thickness (cm)
$\epsilon$	Emittance
$\rho$	Density (gm cm <sup>-3</sup> )
$\sigma$	Stefan-Boltzmann constant (1.355 x 10 <sup>-12</sup> cal sec <sup>-1</sup> cm <sup>-2</sup> K <sup>-4</sup> )

## 1. INTRODUCTION.

Occasional but serious aircraft cabin fires have raised concerns about the fire safety of the materials used in the aircraft interior. Interest has arisen recently for the performance of these materials under fire conditions, which is becoming an important factor in material design and selection. Naturally then the prediction of the performance through thermochemical modeling has emerged as an economic and logical approach in improving fire safety worthiness for its ultimate aim.

The Federal Aviation Administration (FAA) is currently sponsoring modeling activities at the National Bureau of Standards, Harvard University, University of Notre Dame, University of Dayton Research Institute, and Factory Mutual Research Corporation. The present work performed at Jet Propulsion Laboratory (JPL) is but one part of an overall program sponsored by the FAA. Hence, this work complements and does not substitute for the extensive works performed elsewhere.

Unlike the recent study on structural materials (reference 1), the present work is a new direction of the effort to apply some basic thermochemical principles to the combustion of interior materials, such as carpets and seats, under conditions specified by FAA. The specific objective is to predict the burning rates of these materials under pyrolyzing (non-flaming) and flaming conditions. The effects of flame-retarding agents, external radiant heat flux, and pressure change on the burning rates are also studied.

The significance of this work lies in the new concepts introduced, which can be summarized in terms of three fundamental hypotheses:

1. The importance of the condensed phase degradation is emphasized in predicting the burning rates.
2. The degraded matter vaporizing and leaving the surface (vaporize) is specifically described using the vapor pressure equilibrium criterion.
3. The gas phase combustion is treated as controlled by diffusion mixing of oxidizer and fuel and no kinetic considerations may be necessary in many cases of practical interest.

The results obtained from this work are in qualitative agreement with the experimental observations made by FAA. Since the current work is limited to theoretical modeling, a detailed quantitative comparison of the predicted values with experimental results has not been made.

## 2. GENERAL APPROACH.

The thermochemical model used in this work was initially developed (references 2, 3, 4) and applied mainly for the study of behaviour of a class of heterogeneous materials, namely solid propellant combustion. The regression rates of solid propellants predicted by this model were seen to match well with experimental observations. Since the thermochemical performance of interior

materials can be described by the same physico chemical phenomena (i.e., governing equations) as the combustion of propellants, the same theoretical bases are utilized in the present work.

The model differs from those available in the literature in three important aspects. Based on a diverse set of experimental data, the condensed phase degradation is emphasized as the overall rate-limiting reaction. A scientific criterion in specifying the degree of degradation, based on fragment size vaporizing (FSV), is introduced. Lastly, the gas phase reaction is wholly treated as a diffusion (mixing) -controlled process. Since the details are available elsewhere (references 2, 3, 4), only a brief description of the model is given here.

The geometry under consideration is one-dimensional, as shown in Figure 1. In the present work, the steady-state reactions in the condensed phase and gas phase are considered.

### (a) Condensed Phase Details.

The heat input for the condensed phase degradation can be the result of either one or both of two heat fluxes incident on the surface, i.e., one from the flame for which the fuel is supplied by the vaporize from the surfaces, and the other from an external radiation source. The heat is conducted from the surface to the interior, providing the heat needed for the endothermic degradation reaction. The reaction is modeled as a first-order reaction subject to Arrhenius type temperature dependence.

The equation of energy then becomes

$$k \frac{d^2T}{dx^2} + c\rho r \frac{dT}{dx} = D\rho N B \exp(-E/RT) \quad (1)$$

The right hand side of this equation is the heat sink term corresponding to the endothermic first-order degradation reaction described by

$$- \frac{1}{N} \frac{dN}{dt} = B \exp(-E/RT) \quad (2)$$

The symbol N represents the number of bonds per unit mass normalized with respect to that of virgin material.

The boundary conditions for the differential equations are

$$T = T_s \text{ at } x = 0, \quad T = T_0 \text{ at } x = \infty \quad (3)$$

$$N = 1 - \frac{1}{FSV} \text{ at } x = 0, \quad N = 1 \text{ at } x = \infty \quad (4)$$

The symbol FSV stands for fragment size vaporizing, whose importance is well known from earlier works (references 2,3). The formula for FSV was evolved after some study of hydrocarbon vapor pressure data published by the American

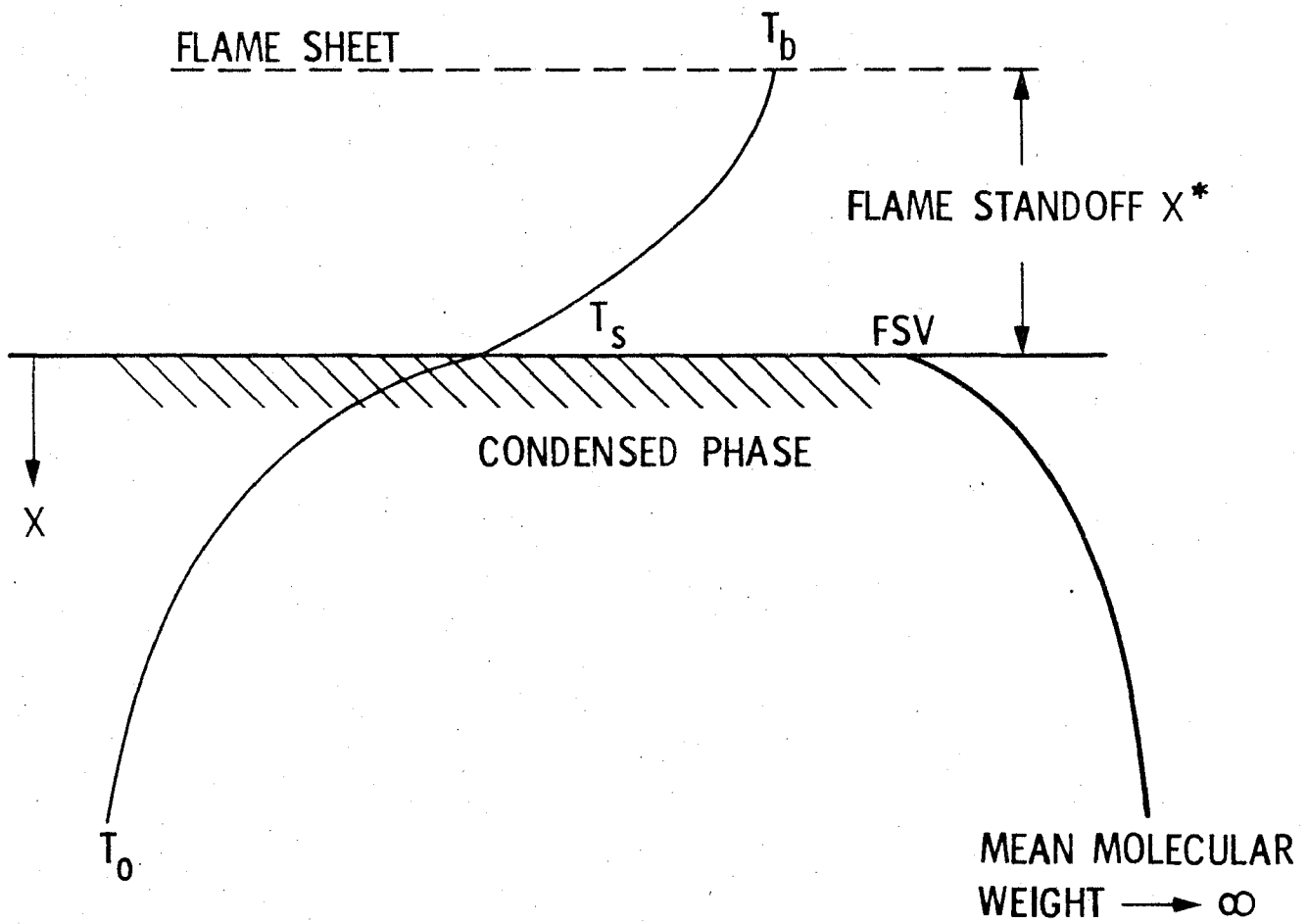


FIGURE 1. THE THERMOCHEMICAL MODEL FOR CONDENSED PHASE DEGRADATION UNDER SHEET FLAME.

Petroleum Institute (reference 5), which predicts the fragment weight of the vaporizate as a function of surface temperature  $T_s$ (K) and pressure P (atm).

$$m = 32.8 P^{-0.2615} \times \exp(3.67 \times 10^{-3} T_s) \quad (5)$$

FSV is obtained after dividing the fragment weight m by the molecular weight of the monomer M. Thus,

$$FSV = m/M \quad (6)$$

The heat flux at the surface to maintain a regression rate r has to be

$$q_s = r\rho c (T_s - T_0) + D\rho r/FSV + \epsilon\sigma T_s^4 \quad (7)$$

The solution for the constant k has been worked out (reference 2) by singular perturbation methods with matching the solutions for the inner (surface) and outer (deep solid) regions. For the steady-state system, the regression rate r is

$$r = \sqrt{\frac{(k/\rho c) B \exp(-E/RT_s)}{\left(\frac{E}{RT_s}\right) \left(\frac{T_s - T_0}{T_s}\right) \left[ \left\{ 1 + \frac{D}{c(T_s - T_0)} \right\} \ln\left(\frac{FSV}{FSV-1}\right) - \frac{D}{c(T_s - T_0)FSV} \right]}} \quad (8)$$

#### (b) Gas Phase Details.

In the gas phase, the flame may or may not appear depending on the condition of heat flux, oxygen concentration and regression rate. In the case where the flame does not appear, the only heat available for the condensed phase degradation is from an external radiation source. In the case where the flame is present, the heat from the combustion zone will be conducted through the gas phase to the condensed phase.

Considering the relatively larger time needed for transport/mixing of oxidizer than the time for the combustion reaction, the flame above the pyrolyzing material is taken as diffusion controlled. Following the familiar flame-sheet approximation, it is modeled that the vapors leaving the surface do not combust until the gases mix well with the oxidizer to reach a distance  $X^*$  (flame standoff distance) from the surface, and they combust completely in a thin zone (flame sheet thickness  $\ll X^*$ ). The temperature of the flame sheet is  $T_b$ .

The energy equation for the region between the flame sheet and the surface is given by

$$k_{gas} \left(\frac{d^2T}{dx^2}\right) + \rho_{gas} c_{gas} U_{gas} \left(\frac{dT}{dx}\right) = 0 \quad (9)$$

The continuity equation is

$$\rho_{\text{gas}} U_{\text{gas}} = \rho r \text{ (from condensed phase)} \quad (10)$$

with boundary conditions

$$T = T_s \text{ at } x = 0, T = T_b \text{ at } x = X^* \quad (11)$$

The solution to equation (9) is

$$q_s = k_{\text{gas}} \left( \frac{dT}{dx} \right)_s = \frac{\rho_{\text{gas}} U_{\text{gas}} (T_b - T_s) \exp(U_{\text{gas}} X^* / \alpha_{\text{gas}})}{1 - \exp(U_{\text{gas}} X^* / \alpha_{\text{gas}})} \quad (12)$$

where  $\alpha_{\text{gas}}$  is thermal diffusivity ( $k/\rho c$ ) of gas.

### (c) Model Predictions.

As can be seen from the solutions, i.e., Equations (8) and (12), there are several input variables needed to compute the regression rate. But most of them are already known or approximated with reasonable accuracy. Thus the most characteristic parameters in this work seem to be the Arrhenius constants, B and E. Values of these constants are obtained using a thermogravimetric analyzer (TGA) as discussed in the next section.

## 3. SUPPORTING EXPERIMENTS.

### (a) Kinetics Constants.

Small scale laboratory experiments were performed to deduce a number of essential input data. The first one was thermogravimetric analysis (TGA). The experiment is to heat up a small sample suspended inside a furnace and record the weight change as a function of temperature. The kinetic constants were deduced then from an Arrhenius plot, a plot of  $\log(-dw/wdt)$  versus reciprocal of absolute temperature. The equipment used in this work was Perkin-Elmer's TGS System 4. By attaching a pair of flowmeters for nitrogen and air to the TGA equipment and varying their flow rates, the effect of oxygen concentration could be studied. The whole system was evacuated with a mechanical pump before purging to ensure a homogeneous atmosphere surrounding the sample.

(1) Wool Carpet (Supplied by the FAA to JPL). The thermogravimetric analysis (TGA) curves for carpet wool are shown in Figure 2. The effect of the presence of oxygen is quite readily seen by comparing the three curves obtained under nitrogen, air and a mixture of 1 percent oxygen and 99 percent nitrogen. Some interesting facts can be observed from this figure. The first one is that, in pure nitrogen, approximately 20 percent of the original mass remains as char at and above 650°C. In air, on the other hand, there is no residue remaining by the time the temperature reaches 700°C. The presence of oxygen from air, however, does not mean the enhanced reaction rates for the entire temperature range. Rather it seems to contribute to preserving the oxidizing

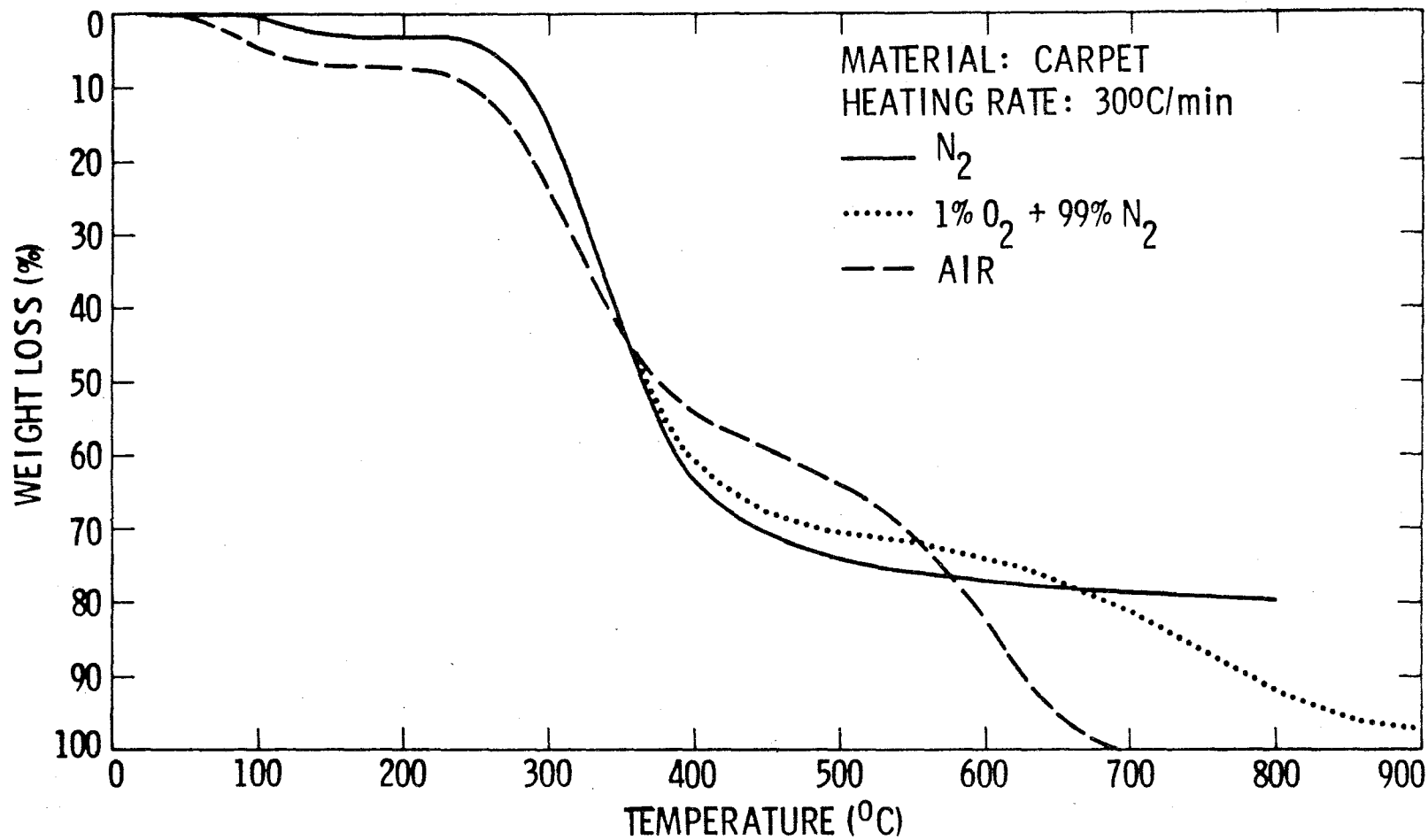


FIGURE 2. THERMOGRAVIMETRIC ANALYSIS OF CARPET FIBERS.

mass temporarily, in this case in the temperature range from 360°C to 575°C. When the oxygen concentration is reduced to 1 percent, the result is the combination of two characteristics, i.e., the carpet behaves like that in pure nitrogen up to 670°C, then burns up almost completely before it reaches 900°C.

This can be elucidated further by using the Arrhenius plot as shown in Figure 3. In pure nitrogen, the degradation reaction takes place in two distinct steps; it increases first and then decreases as the temperature goes higher. For the first step, the conventional Arrhenius expression is

$$r = 7.2 \times \exp(-9,270/RT) \quad T < 641K \quad (13)$$

For the second step, it is

$$r = 3.84 \times 10^{-8} \times \exp(15,000/RT) \quad T > 641K \quad (14)$$

The reaction of the second step might be described as the one with the negative activation energy. But further TGA tests under isothermal conditions show that there are no chain reactions in these high temperature ranges whose termination rates may increase preferentially with temperature to justify the negative activation energy hypothesis. Rather it was found that the wool fibers fuse and coalesce resulting in the decrease of surface area, thus increasing the diffusion and thermal resistances. The SEM (Scanning Electron Microscope) pictures of Figure 4 verify the existence of molten state.

In air, however, the degradation reaction takes place in three steps. In the low temperature region, the reaction rate is the same as that in pure nitrogen. In the medium temperature region, the reaction rate decreases with temperature as in nitrogen, but the rate itself is much lower than in nitrogen. In the high temperature region, the reaction rate increases again with temperature. These observations can be explained in the following way. The degradation in the low temperature region is pyrolysis which is not affected by the presence of oxygen. The lower reaction rates in the medium temperature range seems to be due to the crosslinking caused by oxygen diffusing through the molten phase. The high temperature reaction rate can be simply termed as the char oxidation, expressed by

$$r = 3,300 \times \exp(-22,000/RT) \quad T > 748K \quad (15)$$

(2) Seat Cushion (Polyurethane Foam). Similar tests were performed for seat cushions. The TGA curves are shown in Figure 5 and the Arrhenius plots in Figure 6. As observed in the case of wool, the first phase of degradation of foam in low temperature is the same in air or in pure nitrogen. The difference in reaction rates appears in the next phase. In the absence of oxygen, the degraded foam goes through a melt transition and becomes liquid tar followed by very active boiling-like decomposition (reference 6). In the presence of oxygen, it was observed (reference 7) that the black cellular char is formed and undergoes further oxidation. But the residue of our specimen looked more like tar rather than char. This explains why there is no intermediate transition observed for the foam: the condensed phase material at the surface is a thin layer of liquid tar which does not go through a charring process. (The SEM

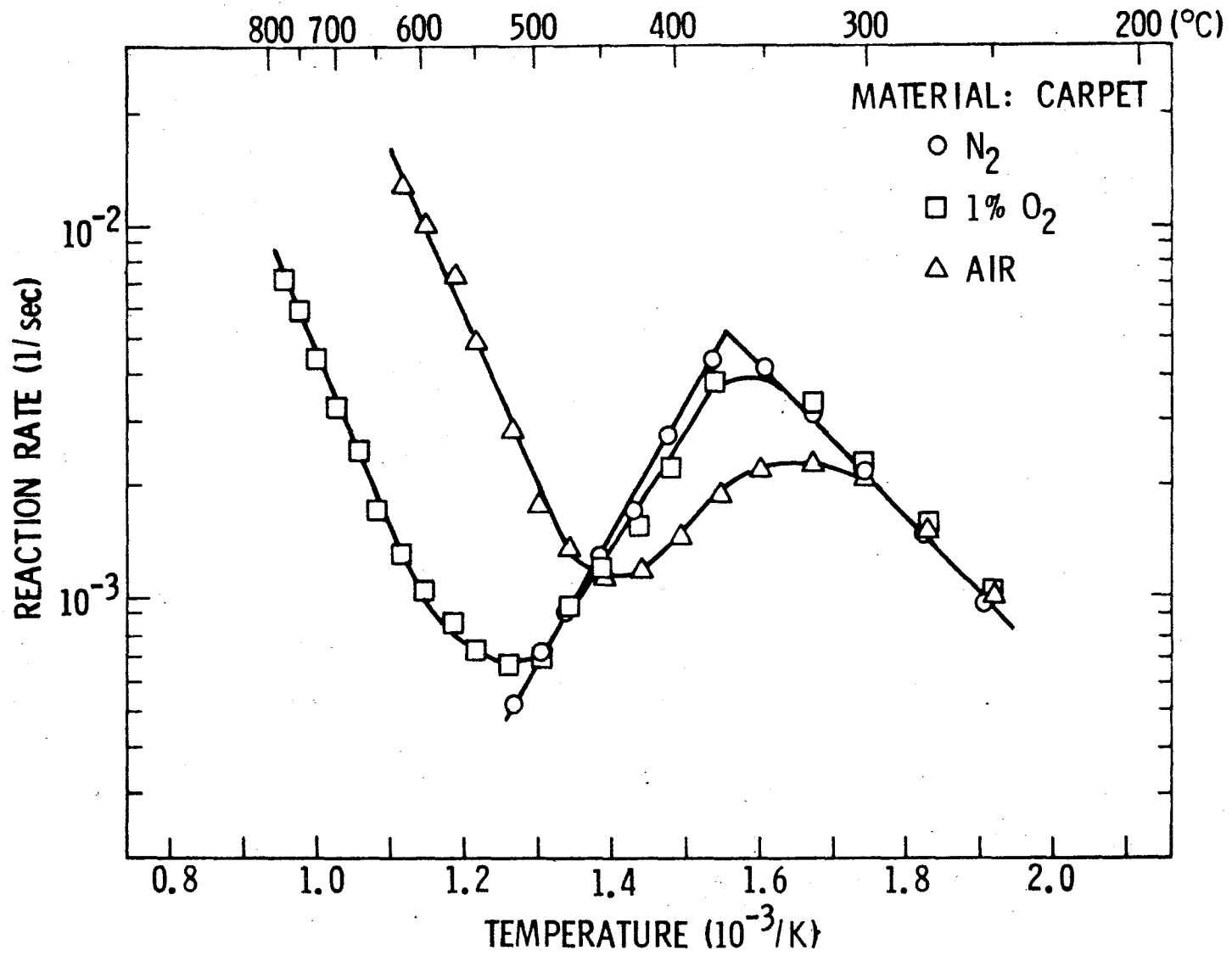


FIGURE 3. REACTION RATE OF CARPET FIBERS DEDUCED FROM TGA.

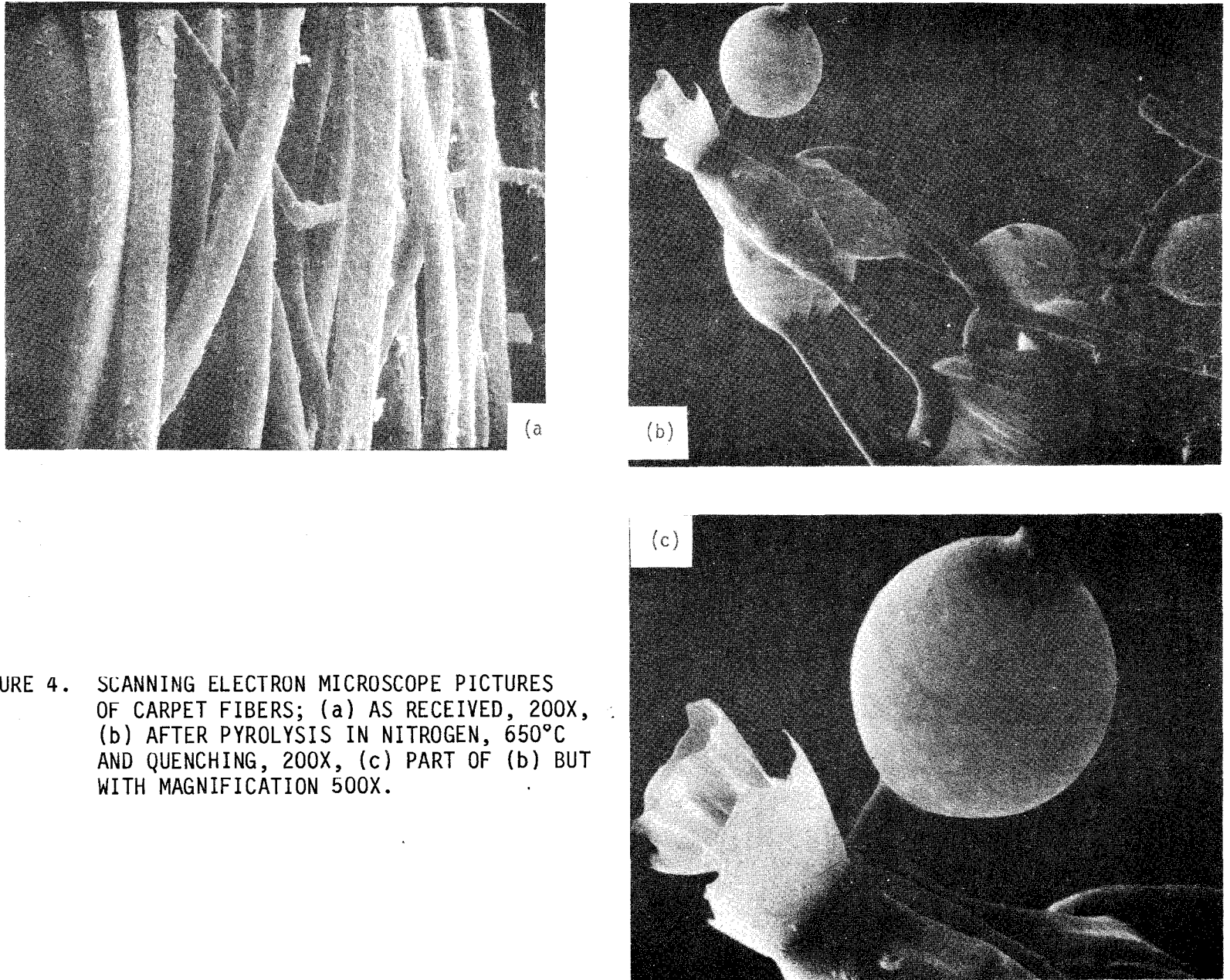


FIGURE 4. SCANNING ELECTRON MICROSCOPE PICTURES OF CARPET FIBERS; (a) AS RECEIVED, 200X, (b) AFTER PYROLYSIS IN NITROGEN, 650°C AND QUENCHING, 200X, (c) PART OF (b) BUT WITH MAGNIFICATION 500X.

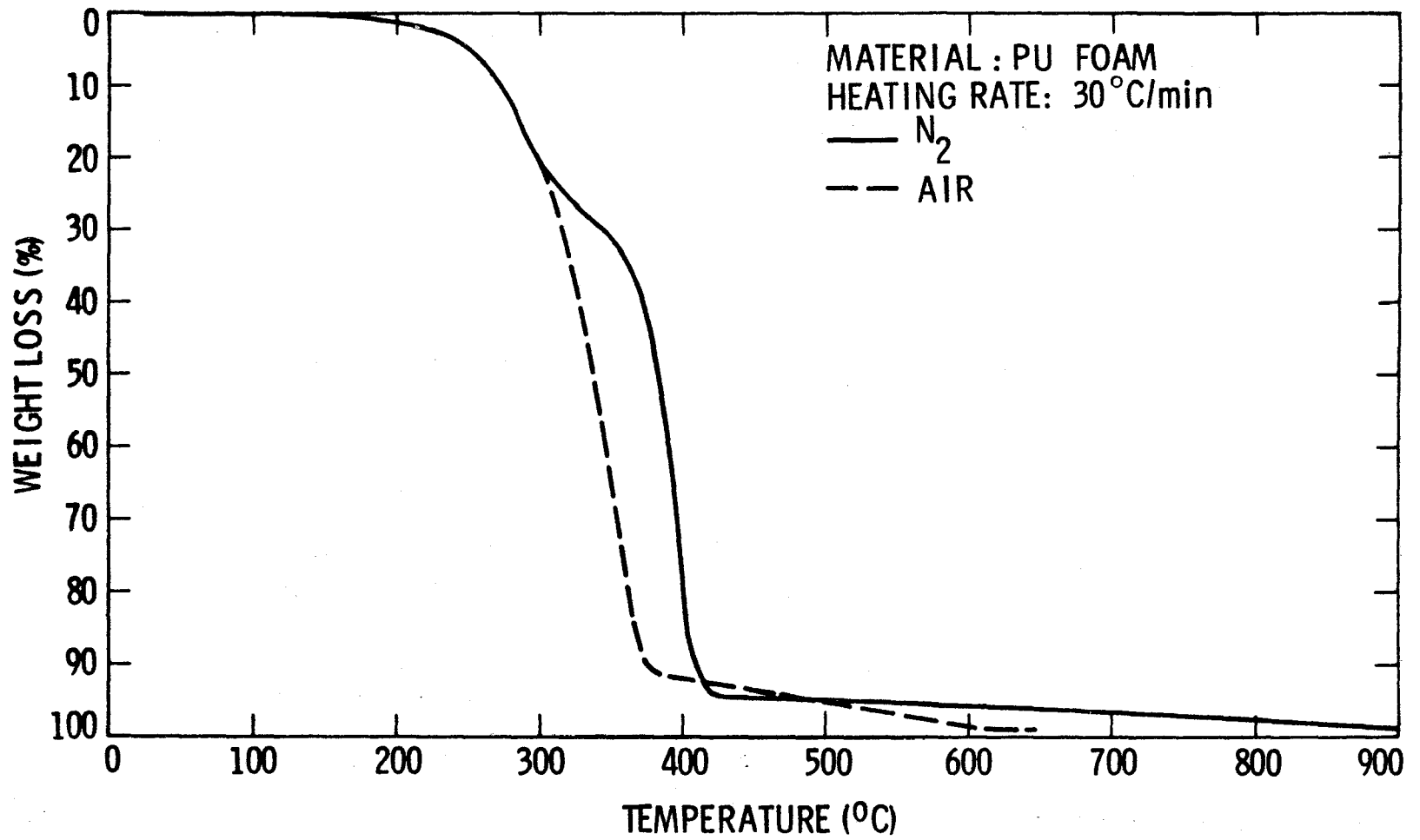


FIGURE 5. TGA ANALYSIS OF SEAT CUSHION (POLYURETHANE FOAM).

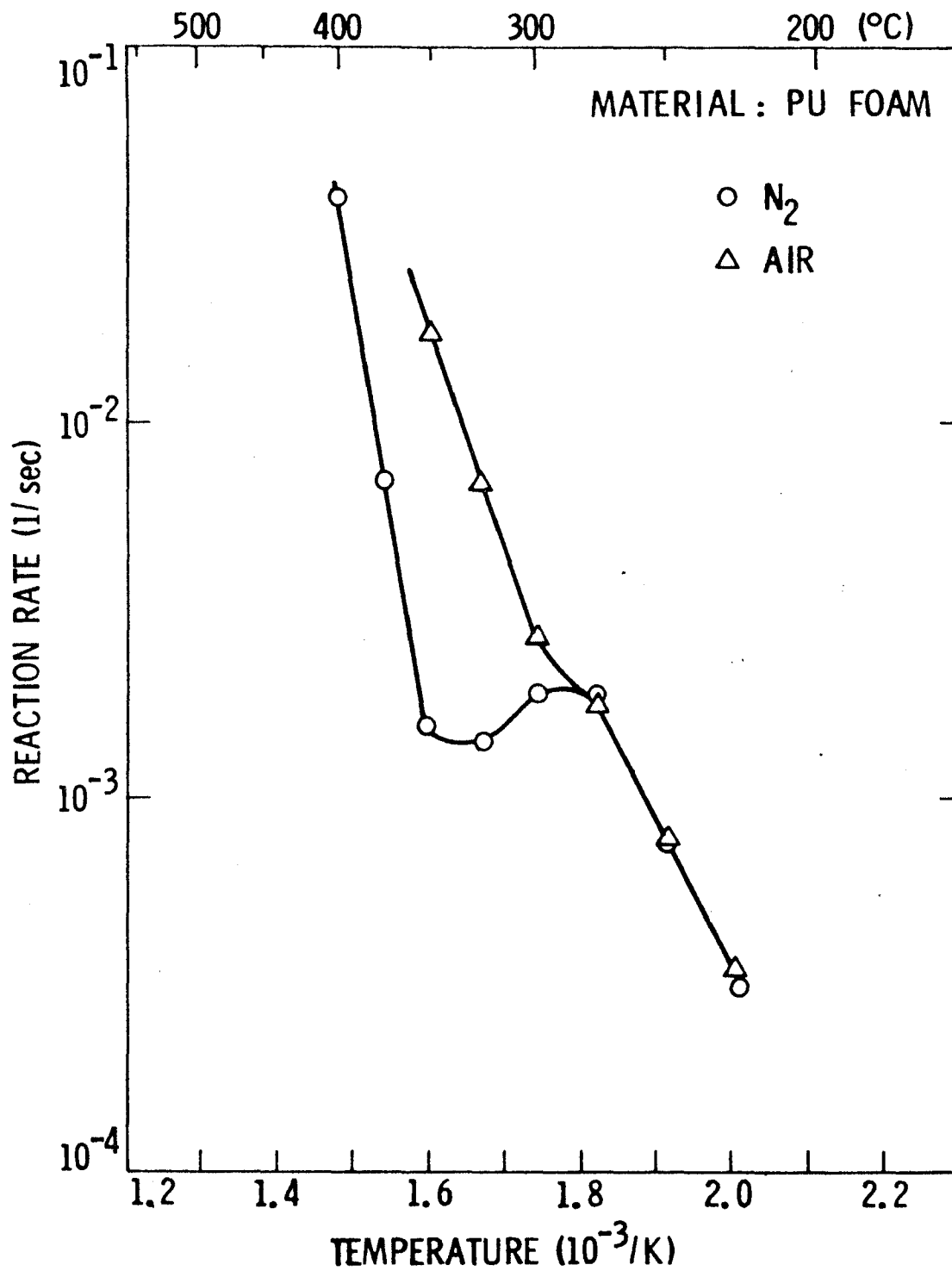


FIGURE 6. REACTION RATE FOR SEAT CUSHION DEDUCED FROM TGA.

show that the melting of wool fibers does not lead to the total agglomeration in any case.)

From the above TGA experiments, the reaction rates of the first phase both in air and in pure nitrogen can be written as

$$r = 95,000 \times \exp(-19,400/RT) \quad T < 548K \quad (16)$$

In pure nitrogen, the reaction rate after phase change can be described as

$$r = 1.9 \times 10^{18} \times \exp(-60,600/RT) \quad T > 623K \quad (17)$$

In air, it can be

$$r = 3.4 \times 10^7 \times \exp(-26,500/RT) \quad T > 573K \quad (18)$$

These results are summarized in Table 1.

#### (b) Other Data.

The current thermochemical model uses rather a small number of input variables, which are thought essential properties of material. Other than the kinetic parameters directly deduced from the TGA experiments, all the properties used in the model are obtained from the literature. These are shown in Table 2.

### 4. SPECIFIC TASKS IN THE INTERAGENCY AGREEMENT.

There were six tasks to be performed by JPL, specified in the Interagency Agreement between FAA and NASA. In this section, the results predicted by the thermochemical model is discussed per each of the six tasks. The first two tasks, however, are discussed under the same head. The computer programs for calculation of the burning rate, heat fluxes required and provided by the flame, and Spalding B number with variable flame standoff distance and ambient pressure are shown in Appendix A for the seat cushion and Appendix B for the carpet.

#### (a) Burning Rates Under Flaming and Non-flaming Conditions.

The first task is to predict the burning rates under the non-flaming condition, with incident radiant heat flux varying between 1 and 14 Btu/ft<sup>2</sup>.sec. The reradiation from the surface is included in the calculation as a source of energy loss. The char layer of the material is assumed to be a diffuse-gray body having the emittance of 0.9.

(1) Carpet. Figure 7 shows the surface regression rates of wool carpet under steady-state non-flaming condition. The rate changes in three distinct segments as the incident radiant heat flux increases. The reason for this distinctiveness is, of course, the change of the activation energy and the pre-exponential factor as discussed in the previous section. It shows that the increasing heat flux does not result in a monotonic increase of the burning rate, but in a sequence of increase-decrease-increase modes. The higher

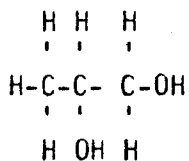
TABLE 1. ARRHENIUS CONSTANTS OBTAINED FROM TGA EXPERIMENTS

Experimental Condition			B Pre-Exponential Factor 1/sec	E Activation Energy cal/g mole
CARPET	N <sub>2</sub>	1st Step, T<641K	7.2	9,270
		2nd Step, T>641K	3.8 x 10 <sup>-8</sup>	-15,000
	Air	1st Step, T<641K	7.2	9,270
		3rd Step, T>748K	3.3 x 10 <sup>3</sup>	22,000
	1% O <sub>2</sub> + 99% N <sub>2</sub>	1st Step, T<641K	7.2	9,270
		3rd Step, T>823K	3.1 x 10 <sup>2</sup>	22,000
SEAT CUSHION	N <sub>2</sub>	1st Step, T<548K	9.5 x 10 <sup>4</sup>	19,400
		3rd Step, T>623K	1.9 x 10 <sup>18</sup>	60,600
	Air	1st Step, T<548K	9.5 x 10 <sup>4</sup>	19,400
		3rd Step, T>573K	3.4 x 10 <sup>7</sup>	26,500

TABLE 2. BASIC DATA USED IN THE CALCULATIONS

	CARPET	CUSHION	GAS PHASE
$\rho$ (g/cm <sup>3</sup> ), net/overall	1.32/0.22	1.05/0.04	ideal gas law
$c$ (cal/g °C)	0.3	0.35	0.3
$k$ (cal/cm °C sec)	0.0001 <sup>a</sup>	0.00034	0.0001 x $\sqrt{T/600}$ <sup>b</sup>
$M$ (monomer Molecular Weight)	138.4 <sup>c</sup>	76 <sup>d</sup>	
$D$ (cal/g)	300	300	
$T_b$ (K)			Carpet: 1400 Cushion: 1400
$T_o$ (k)	300	300	
$\epsilon$	0.9	0.4	
$L$ (cm)	0.8	10.2	

- a. Thermal conductivity of carpet char is taken as  $2 \times 10^{-5}$  cal/cm °C Sec
- b. Calculated according to Sutherland's law
- c. Weight-averaged molecular weight of 17 different amino acids extracted from wool, Ref. 8.
- d. For lack of the information on the specific chemical formulation, the base monomer is assumed to be



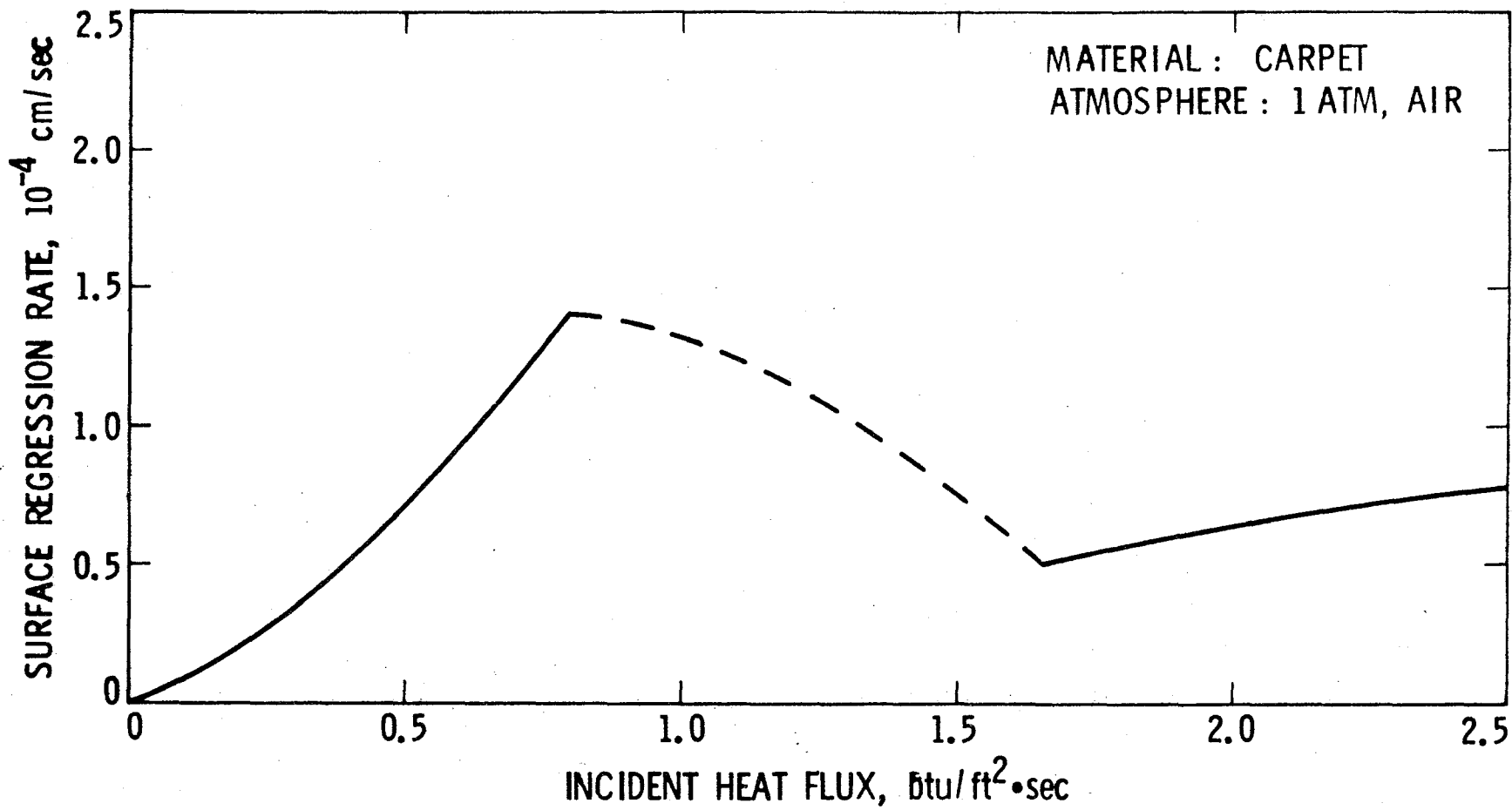


FIGURE 7. THE PREDICTED BURNING RATE OF CARPET WITH INCIDENT HEAT FLUX.

reradiation at the high heat flux region (due to the high surface temperature) reduces the burning rate compared to the rate in the low heat flux region.

The highest temperature region of Figure 7 is studied for the burning rates with self-sustaining flame. The calculation procedure for the burning rate when surface temperature is higher than charring temperature is different from that described earlier. The formation of a char layer causes a substantial reduction of thermal conductivity and hence reduces heat flux through this layer. The temperature profile will be discontinuous at the charring temperature,  $T_c$  (816K for carpet when the atmosphere is a mixture of 1 percent oxygen and 99 percent nitrogen), and a matching condition at this point c becomes

$$q_{c^+} = q_{c^-} \quad (19)$$

$$\text{or} \quad k_{\ell} \left( \frac{\partial T}{\partial x} \right)_{c^-} = k_h \left( \frac{\partial T}{\partial x} \right)_{c^+} \quad (20)$$

Mass continuity requires that the burning rate at the char free surface be equal to the burning rate at the point c under steady-state condition, that is

$$r \text{ at } T_s = r \text{ at } T_c \quad (21)$$

where

$$r \text{ at } T_c = \sqrt{\frac{(k_h/\rho c) B \exp(-E/RT_c)}{\left( \frac{E}{RT_c} \right) \left( \frac{T_c - T_0}{T_c} \right) \left[ \left\{ 1 + \frac{D}{c(T_c - T_0)} \right\} \ln \left( \frac{FSC}{FSC - 1} \right) - \frac{D}{c(T_c - T_0) FSC} \right]}} \quad (22)$$

and

$$r \text{ at } T_s = \sqrt{\frac{(k_{\ell}/\rho c) B \exp(-E/RT_s)}{\lambda \left( \frac{E}{RT_s} \right) \left( \frac{T_s - T_0}{T_s} \right)}} \quad (23)$$

for  $\lambda$  and details of derivation for Eq. (23), the readers are referred to Reference 9. (Note: Eq. (23) is not reduced from Eq. (8). These are solutions to two different problems.)

Thus the burning rate of wool carpet with a char layer on it is determined. Then the heat flux required to maintain this regression rate can be determined by use of Eq. (7), while the heat flux reaching the surface from the flame zone can be obtained by use of Eqs. (10) and (12). These two kinds of heat fluxes are plotted as functions of regression rate in Figure 8.

Figure 8 shows that there exists a special condition under which the carpet is able to sustain its own burning. For steady-state combustion, the heat flux required to produce fuel vapor at the surface must be exactly equal

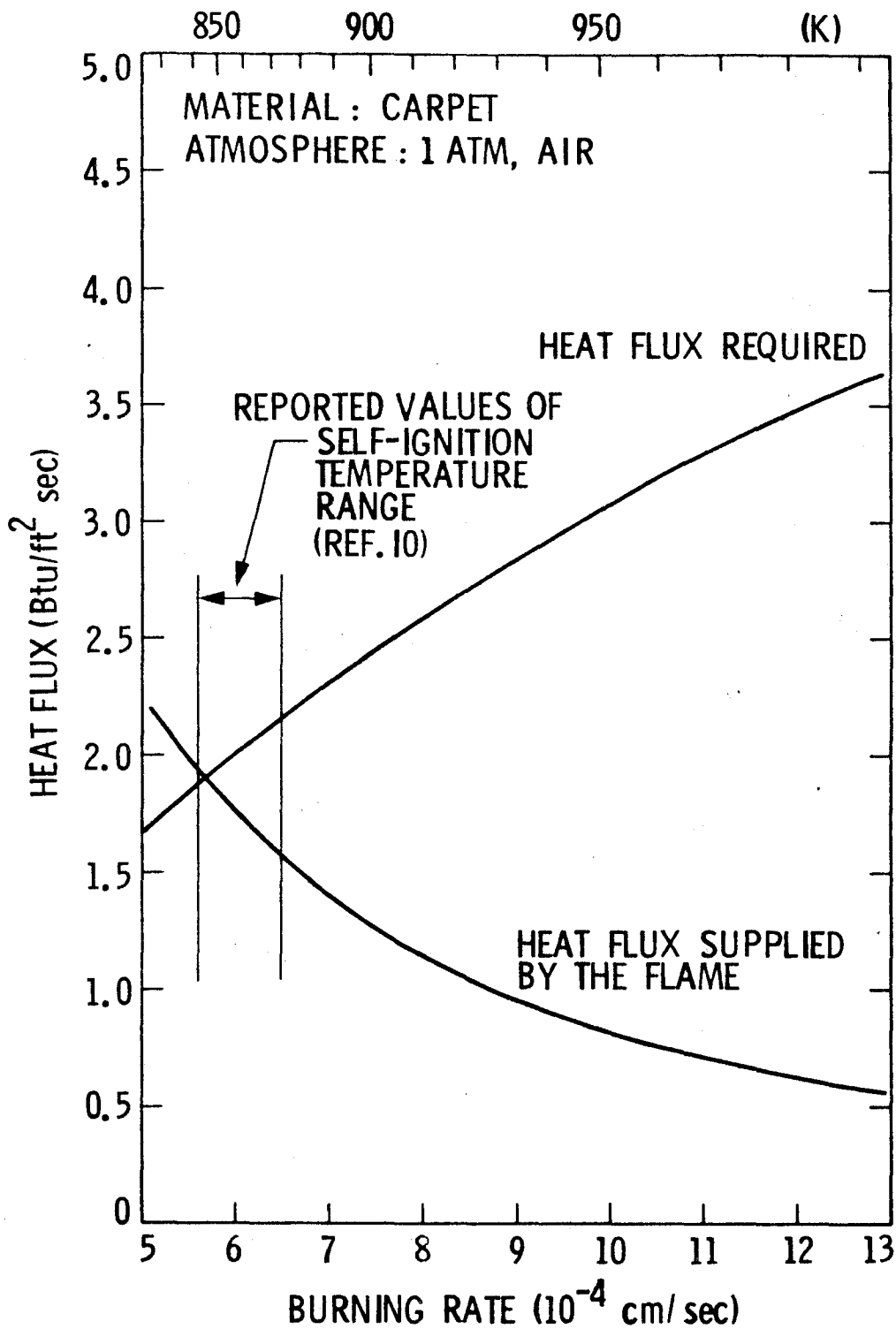


FIGURE 8. THE PREDICTED BURNING RATE OF CARPET.

to the heat flux from the flame generated by combustion of the fuel vapor. The crosspoint of two curves satisfies this condition. So, once this point is reached, the steady-state burning under self-sustaining flame commences. For higher burning rates, however, externally augmented heat flux is needed.

Regarding the actual observations of wool carpet burning, there are two points to be discussed here. The first is that the wool carpet does not get inflamed when a match or even a propane torch is used as an ignition source. The problem with the match fire is that it does not provide enough heat flux to raise the surface temperature for self-ignition. In the case of propane torch, the torch flame covers the surface preventing oxygen in air from mixing with the fuel vapor. The self-sustaining flame was actually observed, however, as shown in Figure 9 when the carpet was heated with the sunlight concentrated by a Fresnel lens (other radiation concentration devices may also be employed). This method has the advantage of providing high heat flux without hindering oxygen diffusion. But the flame disappears, i.e., extinguishes, when the incident radiation beam is blocked or moved away. In other words, the augmenting heat flux is necessary for the wool carpet to burn under a flame. This may seem contradictory to the above description about the self-sustaining flame at the crosspoint of two curves in Figure 8. The reason is the high ignition temperature of wool (reported data: 600°C from reference 10), at which additional 0.6 Btu/ft<sup>2</sup> sec is required from the external radiation heat source. Another reason for the difficulty and hence the sensitivity associated with the existence of flame of wool is due to the high LOI (limiting oxygen index), of which the reported value is 0.252 (reference 11). The LOI is believed to decrease with increasing temperature, so that the flame from wool could be finally observed in air at elevated temperatures, where the oxygen index is 0.21. Such decrease of LOI with temperature was observed for other polymers (reference 12) like polytetrafluoro ethylene, polyvinyl chloride, polymethyl methacrylate, etc.

(2) Seat Cushion. The procedure used for the carpet is applied to the seat cushion material as well. The underlying Arrhenius type reaction rates used in the calculation are those obtained in air, assuming that diffusion of oxygen takes place as in air through the open cell structure of the foam material.

Figure 10 shows the burning rates of seat cushions under flaming conditions. As in the case of the carpet, Figure 10 shows that there exists a condition under which the seat cushion is able to sustain its own burning. The condition is satisfied at the crosspoint of two curves.

#### (b) Effects of Chemical Fire Retarding Agents on Burning Rate

The burning of most polymeric materials proceeds in steps. The first step is the endothermic pyrolysis reaction taking place mostly in condensed phase, and the second step is the exothermic reaction in gas phase. A part of the heat liberated in the second step is transferred to the polymer surface for further cyclic processes.

Chemical fire retardants are those which operate in the condensed phase or in the gas phase to inhibit any of the above reaction steps. The effect of the fire retardant is manifested via physical actions, such as coating on the surface, evolution of non-combustible gases, and absorption of

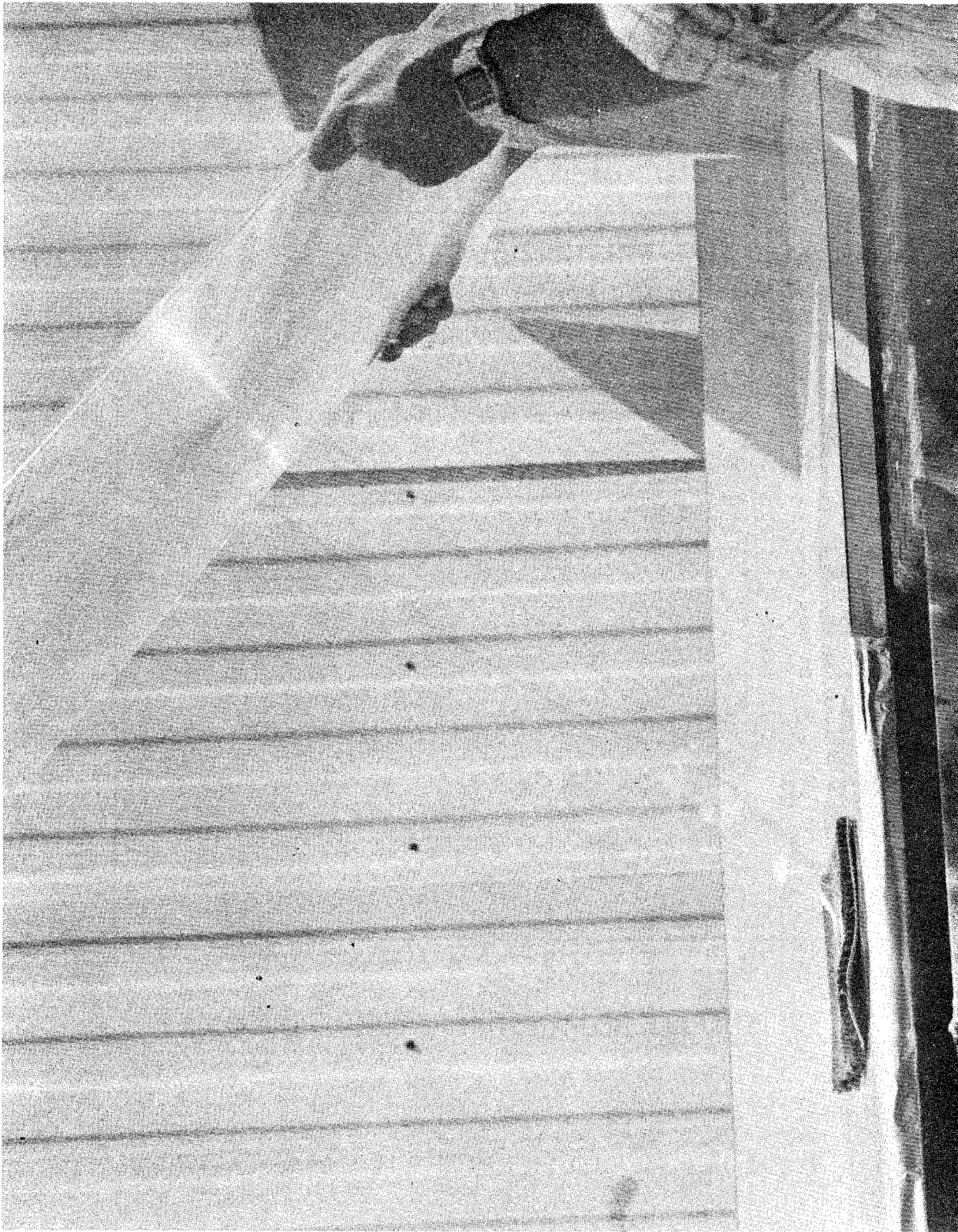


FIGURE 9. THE CARPET UNDER SELF-SUSTAINING FLAME WITH THE SUNLIGHT CONCENTRATION BY A FRESNEL LENS

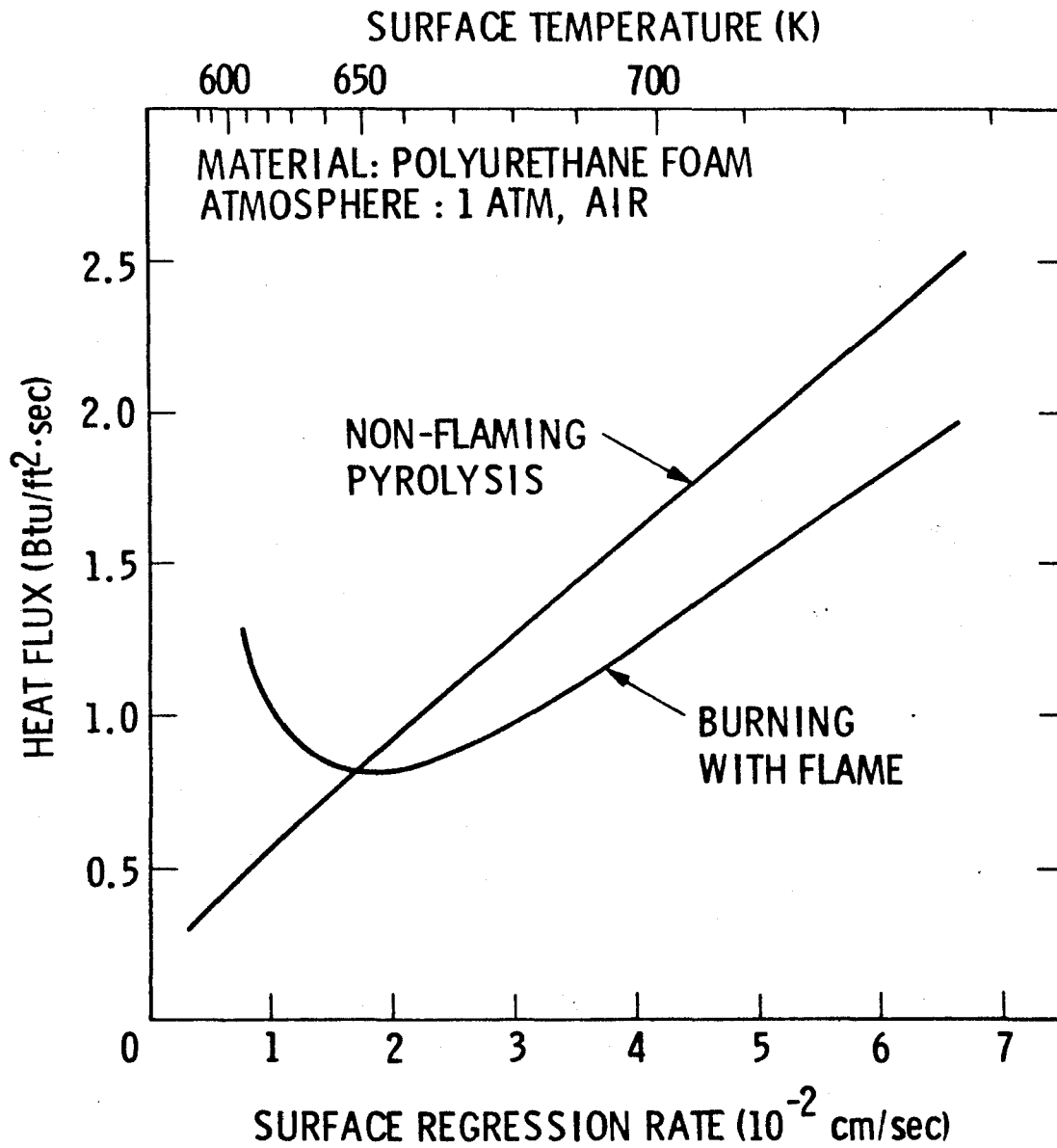


FIGURE 10. THE PREDICTED BURNING RATE OF SEAT CUSHION.

heat, or chemical actions, such as the modification of decomposition reactions, reducing the production of combustible gases, and increasing char formation.

Regarding the thermochemical model used in this work, the effect of the chemical fire retardant can be treated in two ways. If it operates in the condensed phase, the kinetic constants of pyrolysis (B and/or E in Arrhenius expression) will be affected. If it is operating in the gas phase, one or more parameters, such as flame temperature, gas velocity, flame standoff distance, and physical properties of the gas, will be changed.

In order to determine in which phase the fire retardant is effective, the aircraft carpet wool fibers and untreated wool fibers were tested with TGA under  $N_2$  at the heating rate of  $150^\circ C/min$ . The resulting TGA curves show that there is virtually no difference between the flame retardant treated and the untreated wool fibers. In other words, the flame retardant does not affect the condensed phase decomposition reaction. With this particular flame retardant (of which the chemical composition is not known to us) applied to the aircraft carpet wool, it is reasoned that the flame retardancy takes place in the gas phase.

In the case of the seat cushion material, this type of TGA experiment to single out the effect of the flame retardant is not feasible, because of the difficulty in obtaining exactly the same material in a pair, i.e., one treated with a flame retardant and the other untreated.

Without having detailed information on the flame retardants actually used and their physical/chemical effect on gas phase reactions, the current model assumes a modified value (increased by 20 percent) of flame standoff distance as a surmised effect of the flame retardant. The flame temperature is another parameter that can be modified (lowered), but this change is equivalent to the change of the flame standoff distance for the present purpose.

The predicted results are shown in Figure 11 for the carpet and Figure 12 for the seat cushion. These are similar to the curves seen in Figures 8 and 10 except that the heat fluxes supplied from the flame are lowered because of the increased flame standoff distance. Hence for the case of wool carpet, the heat required from an external radiation source to start burning under flame is larger, making the ignition more difficult. This is the situation predicted using the same ignition temperature as that of untreated wool fibers. If the ignition temperature is increased due to the flame retardants, then the augmenting heat flux will be even larger. For the case of the seat cushion material, the same reasoning as for the wool carpet will hold. The ignition temperature of the urethane foam is not available in literature, and is not pursued in this work.

(c) Integration of the Nomenclature: "Thermal Thickness" and "Thermal Thinness".

The thermochemical model used in this work has been developed for and hence is applicable to a thermally thick material. The term "thermally thick" or "thermally thin" is used in comparison with the physical thickness  $L$ . So, when the physical thickness  $L$  is larger than the thermal thickness  $\delta$ , it is

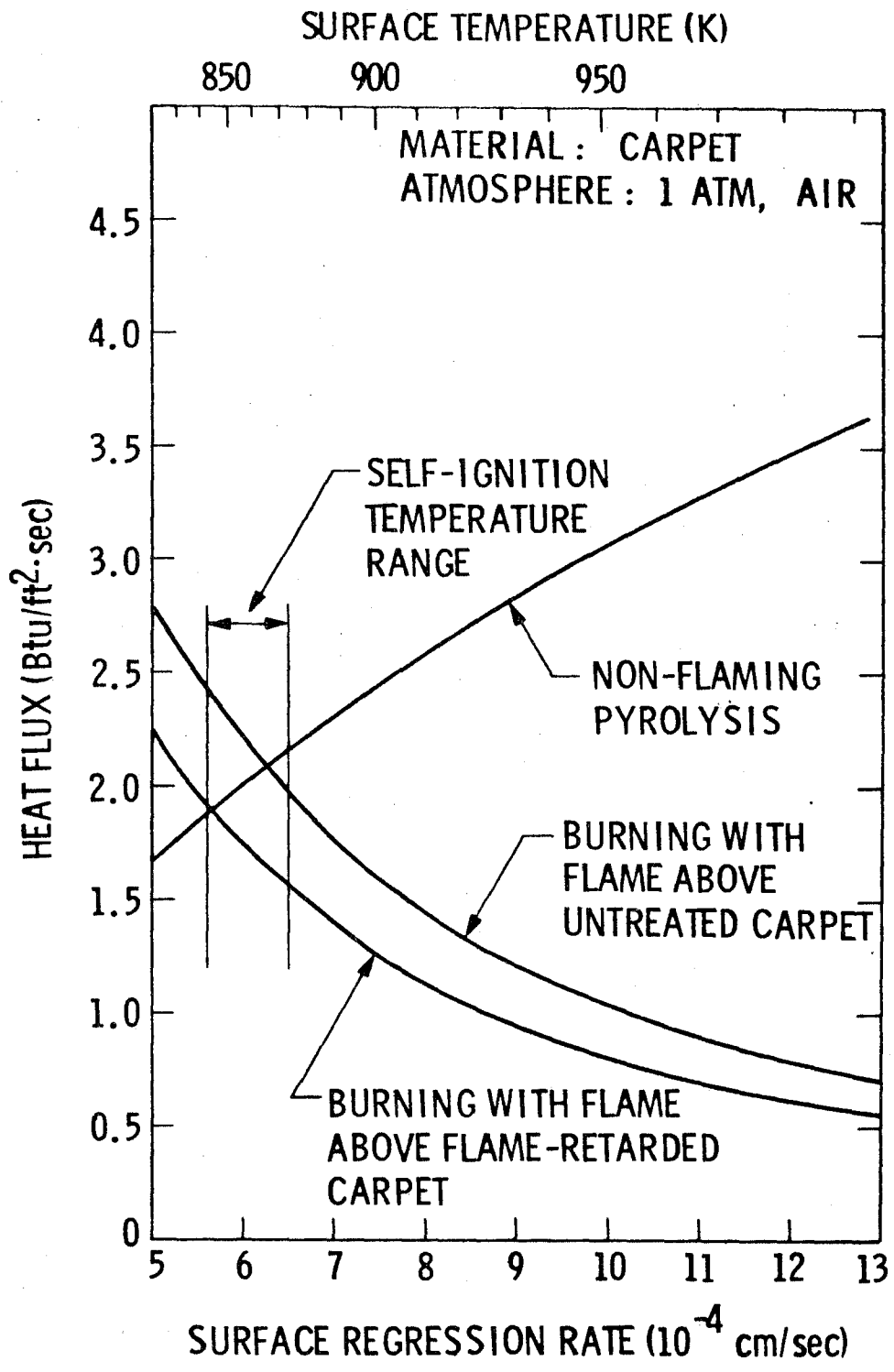


FIGURE 11. THE PREDICTED EFFECT OF FLAME-RETARDANT ON THE BURNING OF CARPET.

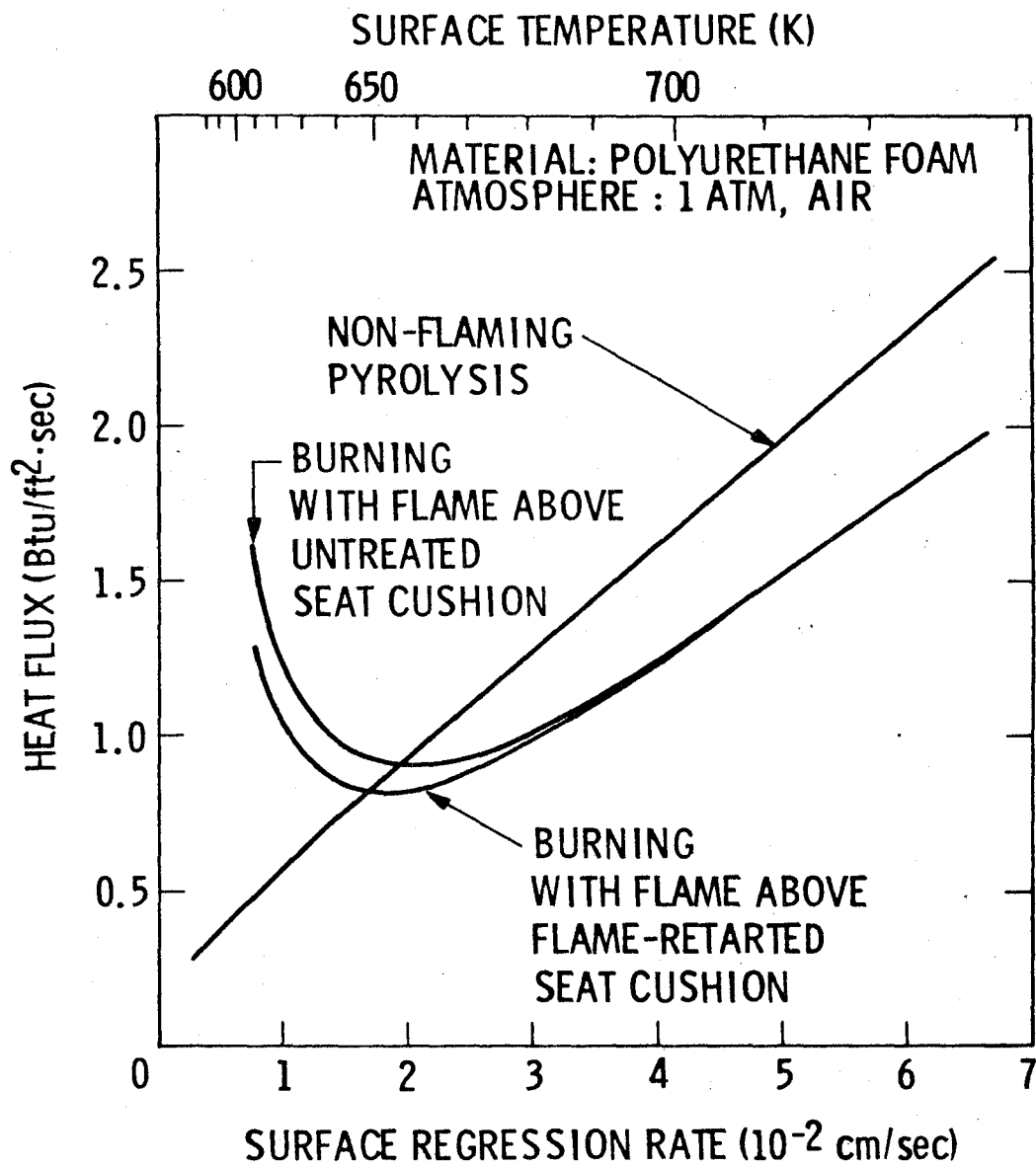


FIGURE 12. THE PREDICTED EFFECT OF FLAME-RETARDANT ON THE BURNING OF SEAT CUSHION.

called "thermally thick", otherwise "thermally thin", i.e.,

$$\begin{aligned} \delta &\ll L \text{ thermally thick} \\ \delta &\gg L \text{ thermally thin} \end{aligned}$$

The  $\delta$  can be deduced (reference 2) from the outer region (cold side) temperature profile of a slab whose other side is heated. That is,

$$\frac{T-T_0}{T_s-T_0} = \exp(-xr/\alpha) \quad (24)$$

where  $\alpha$  is the thermal diffusivity.

$$\text{Then } x = -\frac{\alpha}{r} \ln \left( \frac{T-T_0}{T_s-T_0} \right) \quad (25)$$

The thermal thickness  $\delta$  is defined as the depth from the surface where the dimensionless temperature  $(T-T_0)/(T_s-T_0)$  is equal to  $1/e$ .

$$\text{or } \delta = \frac{\alpha}{r} = \frac{k}{\rho c r} \quad (26)$$

In the calculation of  $\delta$  for the carpet, the data of the thermal conductivity, density, and heat capacity used are for the carpet char layer because this is where most of the temperature drop occurs and hence thermal resistance is provided. For seat cushion, the calculation is straight forward.

With the physical properties listed in Table I, it can be seen that

$$\begin{aligned} \delta &< L \text{ for carpet} \\ \delta &\ll L \text{ for seat cushion} \end{aligned}$$

In other words, both materials can be regarded as thermally thick. If the physical thickness ( $L$ ) is reduced and becomes smaller than thermal thickness ( $\delta$ ), the material is considered thermally thin. For a thermally thin material, the burning rate can be calculated directly from the Arrhenius rate equation,

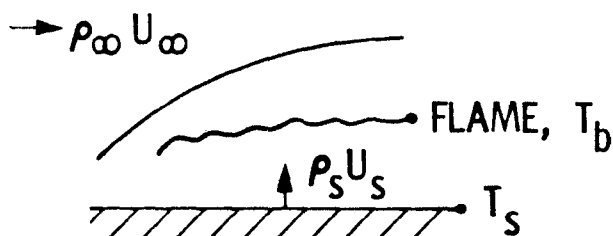
$$r = L B \exp(-E/RT_s) \quad (27)$$

It should be appropriate to note here that the thermal thickness ( $\delta$ ) of the carpet changes with the progress of thermal degradation, due to the change of  $k$  and  $r$ . Before the char layer is formed at the surface, the same calculation shows that the entire carpet is thermally thin. But after the charring, largely due to the change in  $k$ , the carpet has become a thermally thick material. A detailed study of this effect can be found in Reference 9.

#### (d) Relating the Vaporization Concept to the Spalding B Number.

This task is to study the effect of convective flow over the burning surface on the burning rate of the condensed phase. The geometry under consideration is depicted in Figure 13. At a distance away from the leading edge of burning surface, the heat flux to the condensed phase is

$$k \left. \frac{\partial T}{\partial x} \right]_{x=0} = (\rho U)_\infty c (T_b - T_s) C_H \quad (28)$$



DEFINITION:

$$B = \frac{(\rho U)_s}{(\rho U)_\infty C_H}$$

FIGURE 13. THE SCHEMATIC DIAGRAM FOR THE CONDENSED PHASE BURNING WITH CONVECTIVE FLOW.

where  $C_H$  is the Stanton number, and  $(\rho U)_\infty$  is the mass flow rate at the outer edge of the boundary layer at that location. The mass transfer number  $B$ , (or Spalding  $B$  number) is defined by

$$B = \frac{(\rho U)_s}{(\rho U)_\infty C_H} \quad (29)$$

where  $(\rho U)_s$  is the mass burning rate at the surface. Since  $C_H$  is the reduced heat transfer coefficient due to the burning mass injection, frequently it is assumed that Reynolds analogy holds and hence,

$$\frac{C_H}{C_{H_0}} = \frac{C_f}{C_{f_0}} \quad (30)$$

where  $C_f$  is the skin friction coefficient and  $C_{H_0}$  and  $C_{f_0}$  are, respectively, Stanton number and friction factor without mass injection to the flow.

Further analysis (reference 13) shows that the ratio of Stanton numbers can be approximated as

$$\frac{C_H}{C_{H_0}} = \frac{\ln(1+B)}{B} \quad \text{for } B < 5 \quad (31)$$

$$\frac{C_H}{C_{H_0}} = 1.2 B^{-0.77} \quad \text{for } 5 < B < 95 \quad (32)$$

and

$$C_{H_0} = \frac{C_{f_0}}{2} = 0.12 \text{ Re}^{-0.2} \quad (33)$$

where Re is the Reynolds number based on the distance from the leading edge of burning surface. The Spalding B number is calculated after rearranging Eqs. (29) and (31) or (32) to give

$$B = \exp \left\{ \frac{(\rho U)_s}{(\rho U)_\infty C_{H_0}} \right\} - 1.0 \quad \text{for } B < 5 \quad (34)$$

or

$$B = \left\{ \frac{(\rho U)_s}{1.2 (\rho U)_\infty C_{H_0}} \right\}^{1/0.23} \quad \text{for } 5 < B < 95 \quad (35)$$

The Spalding B number calculated for carpet ranges from 0.17 to 0.18 at surface temperatures of 830 to 850K, at 2 feet downstream from the leading edge of the burning surface, and at 3.0 mile/hr blowing velocity of free stream. The value of B number is comparable to that of carbon (reference 14), i.e., 0.12, but easier to burn than the carbon. However, in order to make the carpet actually burn, more additional heat flux is needed from an outside source. In other words, the effect of the flow is such that there will be no burning with a self-sustaining flame but only smoldering.

Under the same condition, the Spalding B number for seat cushion is 1.13 at the surface temperature of 650K, where the burning can proceed with the self-sustaining flame. The relatively high value of B compared to that of carpet is because of the high reactivity of seat cushion as shown from the TGA experiments (see Table 1).

#### (e) Effect of Pressure on Burning Rates.

The effect of changing pressures were studied since the pressure affects the ignition/combustion process in several ways. The most obvious is the effect on vapor density ( $\rho = PM/RT$ ) and the vapor phase chemical kinetic rates that are frequently approximated by  $P^n$  where n is the "index" of reaction rates.

In our particular thermochemical model the pressure affects two important characteristics. Firstly, under the basic hypothesis of heterogeneous condensed phase reactions by an autocatalytic species (probably the cure catalyst), the condensed phase pre-exponential factor B is directly proportional to the mean pressure. That is, B takes the form of  $B \times P$ , where P is in atmospheres. Secondly, under the novel vapor pressure equilibrium criterion used here, pressure affects the mean molecular weight of the vaporizing species, namely the pyrolysis products. So, FSV is modified by a factor of  $P^{-0.2615}$ , as shown in Equation (5). These separate effects are believed here to be very essential for a complete understanding of the pressure effects. It is also thought that highly simplified approaches may ignore the main point of the negative effect of pressure that has sometimes been observed in fire phenomena.

The results show that the pressure increase does increase the burning rate in a monotonic way, as shown in Figure 14 for carpet and Figure 15 for seat cushion. The burning rates of these curves are those obtained under the steady-state self-sustaining flames. So, additional incident heat flux will increase the burning rates accordingly. As shown in these figures, the pressure dependence is far weaker than a direct (linear) dependence. The curves here do indicate the basic thoughts behind pressure scaling (modeling) of fires in experimental facilities.

## 5. CONCLUSIONS.

The present work on the prediction of thermochemical performance of carpet and seat cushion leads to the following conclusions.

1. The assumption of condensed-phase degradation as the rate-limiting step in the model leads to theoretical results which match qualitatively with experimental observations.
2. The application of vapor pressure equilibrium criteria appears to be a valid procedure in removing the arbitrariness in the description of the vaporization step at the surface.
3. Although it was satisfactory in the present work, a further understanding of the flame standoff distance and heat flux therefrom seems necessary, especially for the slow burning materials like the carpet.
4. As an overall summary, the specific objective of predicting the burning rates as a function of the material properties was accomplished with qualitative agreement with experiments.

Up to this point, the theoretical results have not been tested with quantitative experimental measurements. In order to appreciate the validity of the model, actual burning rate measurement is necessary after re-evaluating the fundamental physical and thermal properties of the material used in the calculation. In fact, some of the property values were taken from the literature and may not be correct for the specific material in consideration.

## 6. FUTURE WORK.

The extension of the present work is planned for a more practical case of multi-layered polymeric materials, namely a system consisting of polyurethane foam (cushion) - neoprene sheet (blocking layer) - nylon/wool fabric (cover). Also planned is the experimental measurement of thermochemical performance of the system using a modified NBS Smoke Chamber. A Mellen furnace is to provide radiant heat flux varying from 2 to 10 Btu/ft<sup>2</sup> sec and the resultant weight loss and temperature profile in the material will be measured. The kinetic constants of the individual material deduced from TGA experiments along with other thermal data will be integrated into the model and its prediction compared with the observed results. This work is scheduled to commence shortly under the sponsorship of the FAA.

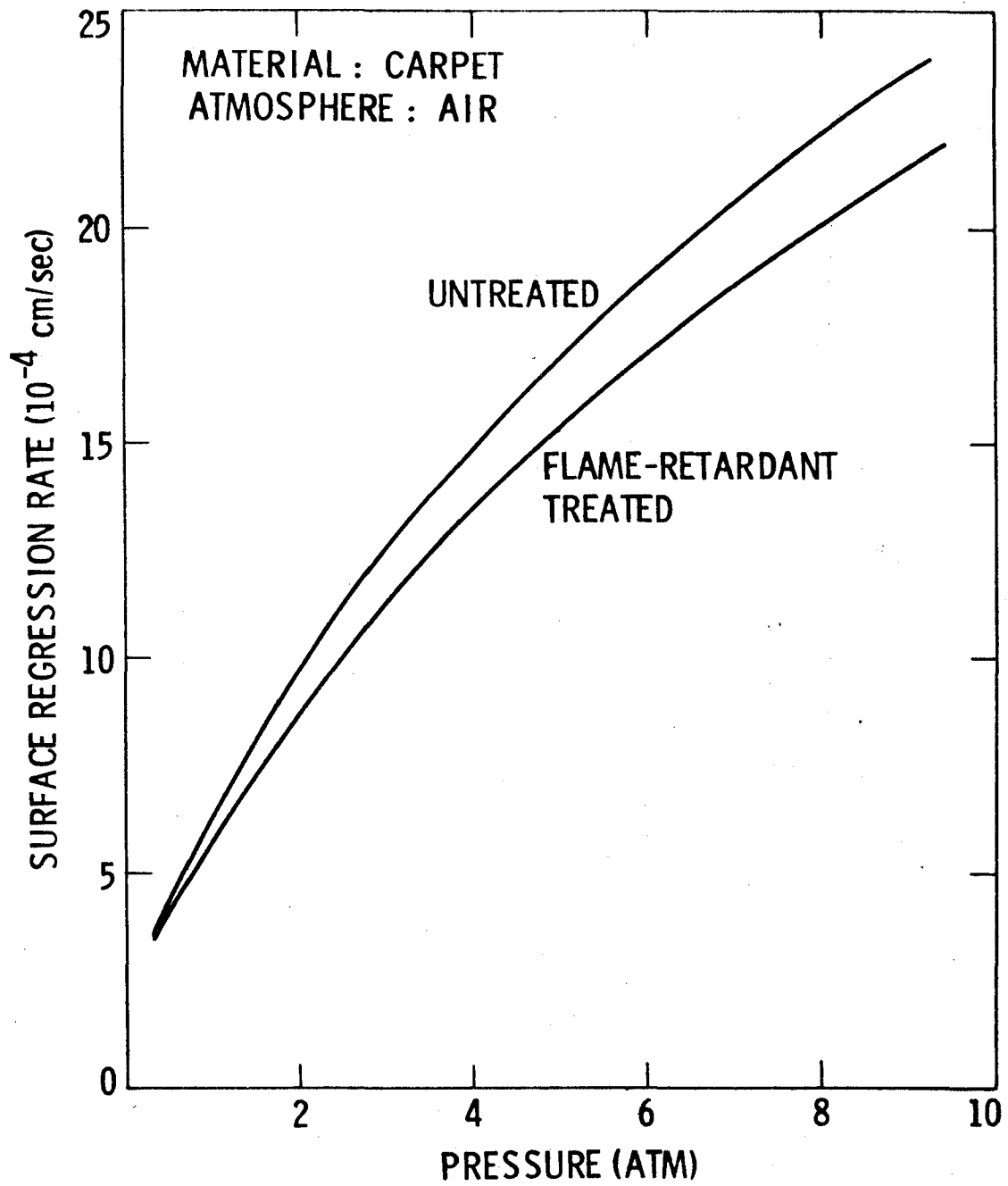


FIGURE 14. THE PRESSURE DEPENDENCE OF BURNING RATE OF CARPET.

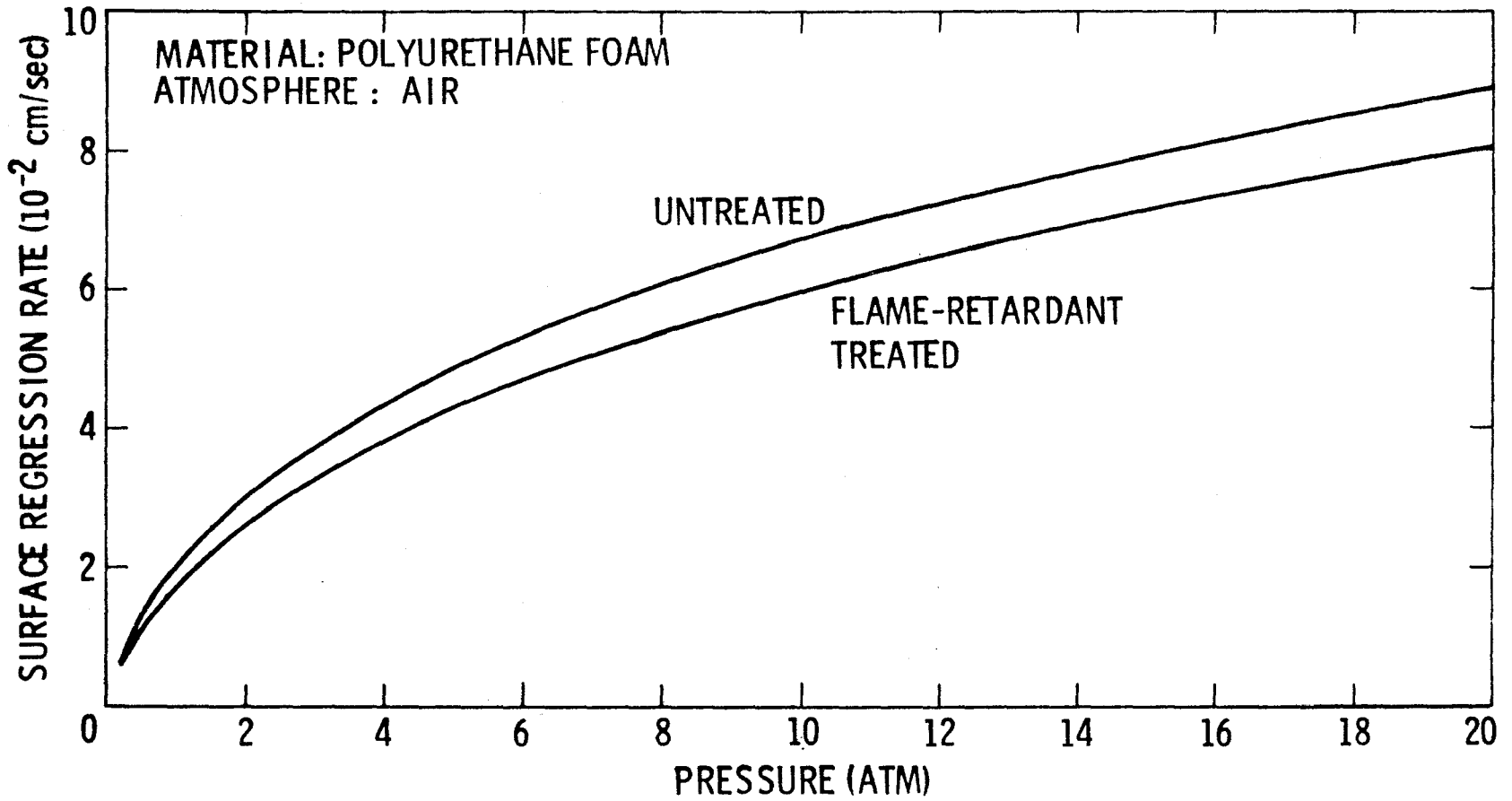


FIGURE 15. THE PRESSURE DEPENDENCE OF BURNING RATE OF SEAT CUSHION.

## REFERENCES

1. Ramohalli, K and Sahakian, J.: Parametric Results for Heat Transfer Across Honeycomb Sandwich Panels, AIAA 19th Aerospace Sciences Meeting, Paper No. AIAA-81-0213, St. Louis, MO., January 1981.
2. Kumar, R. N. and Stickler, D. B.: Polymer Degradation Theory of Pressure-Sensitive Hybrid Combustion, XIII Symposium (International) on Combustion, The Combustion Institute, 1971, pp. 1059-1072.
3. Kumar, R. N.: Condensed Phase Details in the Time-Independent Combustion AP/Composite Propellants, Comb. Sci. and Tech., Vol. 8, No. 3, pp. 133-148, 1973.
4. Kumar, R. N. and Culick, F. E. C.: Role of Condensed Phase Details in the Oscillatory Combustion of Composite Propellants, Comb. Sci. and Tech., Vol 15, pp. 179-199, 1977.
5. American Petroleum Institute: Technical data book - Petroleum Refining, Chapter 5, 1966.
6. Varney, A. M. and Strahle, W. C.: Thermal Decomposition Studies of Some Solid Propellant Binders, Combustion and Flame, Vol. 16, pp. 1-8, 1971.
7. Rogers, F. E., Ohlemiller, T. J., Kurtz, A. and Summerfield, M.: Studies of the Smoldering Combustion of Flexible Polyurethane Cushioning Materials, J. Fire and Flamm., Vol. 9, pp. 5-13, 1978.
8. Seifter, S. and Gallop, P. M.: The Structure Proteins, in The Proteins-Composition, Structure and Function, Vol. 4, ed. Neurath, Hans, p. 317, Academic Press, 1966.
9. Ramohalli, K. and Mink, M.: Thermal Performance Modification of Composite Materials, AIAA 17th Aerospace Sciences Meeting, New Orleans, Louisiana, January, 1979, Paper No. 79-0018.
10. Crawshaw, G. H., Duffield, P. A. and Mehta, P. N.: J. Appl. Polym. Sci., Applied Polymer Symposia, No. 18, Proc. 4th International Wool Textile Conference, part II, p. 1183, 1971.
11. Benisek, L.: Flame Retardance of Protein Fibers, Chapter 3 in Lewin, M., Atlas, S. M. and Pearce, E. M. eds., Flame-Retardant Polymeric Materials, Plenum Press, N. Y., 1975.
12. Fenimore, C. P.: Candle-type Test For Flammability of Polymers, Chapter 9, *ibid.*
13. Marxman, G. A., Wooldridge, C. E. and Muzzy, R. J.: Fundamentals of Hybrid Boundary-layer Combustion, Preprint 64-505 at the AIAA Heterogeneous Combustion Conference, Palm Beach, FLA., December, 1963.
14. Glassman, I., Combustion, Academic Press, 1977, pp. 183.